

A direct numerical simulation study of a turbulent lifted flame in hot oxidizer

Shahram Karami¹, Evatt R. Hawkes^{1,2} and Mohsen Talei²

¹School of Photovoltaic and Renewable Energy
The University of New South Wales, Sydney, 2052 AUSTRALIA

²School of Mechanical and Manufacturing Engineering
The University of New South Wales, Sydney, 2052 AUSTRALIA

Abstract

This paper presents a Direct Numerical Simulation (DNS) study of the stabilisation of a turbulent lifted flame in hot oxidizer, a problem of practical significance in diesel engines, gas turbines, and recirculating industrial burners. A slot jet of fuel issuing into a hot co-flow oxidizer stream is simulated using a single-step chemistry model and assuming unity Lewis number. A jet Reynolds number of 5,300 was enabled by the use of scalable high-order numerical methods and highly parallel computation. The basic structure of the flame is described noting features of the flame base and trailing premixed and diffusion flames. The flame base is studied to determine whether the stabilisation is due auto-ignition, premixed flame propagation, or another mechanism. The flame index (FI) is used to distinguish non-premixed flames from premixed flames close to the flame base. The time evolution of temperature, reaction rate and scalar dissipation rate along with iso-lines of appropriate temperature and most reactive mixture fraction are analysed to identify the flame base. It is concluded that the flame base exists on the outer boundary of the jet and consists of mainly non-premixed flames followed by a vigorous trailing rich premixed flame region inside the jet.

Introduction

A lifted non-premixed flame is one of the flame distinguishable configurations which has been repeatedly observed in industrial and commercial engineering devices (e.g. steam boilers). When the flame is attached to the hot burner rim, the stabilisation process is clearly understood [1]. However, in industrial burners and in diesel engines, the high jet exit velocities cause a lifted flame which is stabilised downstream of the nozzle exit. In the lifted flame, the flame base experiences interaction of chemistry and turbulence which makes the stabilisation process more complicated compared to an anchored flame and therefore, needs to be understood. The main advantage of having a lifted flame is reduction in heat transfer back to the burner. In the case of anchored flames, significant heat transfer to the burner necessitates the use of expensive high-temperature resistant materials, such as ceramics. However, commonly available metals can be used for construction of lifted flame burners which means simple manufacturing and therefore lower production costs. Another advantage of using lifted flames is the reduction of emissions as a result of enhanced mixing prior to combustion.

Recently, fundamental studies of turbulent non-premixed jet flames have received increased attention. The distance of flame from the nozzle, which is referred to as 'lifted length', is sensitive to the flow conditions. In some circumstances, rapid extinction and re-ignition may occur, having a high impact on combustion stability. As a result, turbulent lifted flame stabilisation is a central interest in combustion research now. Several 3D DNS studies of turbulent lifted flames considering detailed chemistry have been performed. For instance, unsteadiness of

the flame and formation of the diffusion flame islands in a hydrogen jet flame was studied by Mizobuchi *et al.* [4]. The flame index (FI) [16] and mixture fraction were used to distinguish the leading edge flame, the inner rich premixed flame and outer diffusion flame islands. Yoo *et al.* [5] investigated a turbulent lifted hydrogen slot-burner jet flame in a heated co-flow using DNS. In this study, the location with $Y_{OH} = 0.001$ coincides with the increase of temperature, commencement of heat release, build up of the high temperature radical pool and vanishing of HO_2 . Therefore, this isoline was used as a marker of the flame base. Based on instantaneous images of HO_2 and OH , the authors concluded that the main reason of flame stabilisation when the co-flow temperature was chosen to be higher than the cross-over temperature was auto-ignition. As temperature and OH concentration had a local maxima, it was concluded that auto-ignition occurs locally. Statistics of FI and Damköhler number Da revealed that auto-ignition occurred in lean mixtures where the fuel gradient and oxidizer gradient were opposed. In a separate study, Yoo *et al.* [6] performed DNS of 3D turbulent ethylene lifted flame jet in a highly heated co-flow using a reduced chemical kinetic mechanism. Hydroxyl was used as the marker of the lifted flame base and ignition kernels were marked with high OH concentration. From analysis of the flame structure, the authors concluded that auto-ignition was once again the main mechanism of stabilisation.

The simulation of Yoo *et al.* [6] needed 14 million CPU-hours (20 days on 30000 processors) and 250 TB storage space. Taking into account the computational resources which have been used for these simulations, it can be concluded that the detailed chemistry modelling of 3D lifted flames are presently limited to a few cases and it is rarely possible to study comprehensively the effect of chemistry and flow parameters on flame structure. Thus, while the above works have provided useful insights, they do not span a sufficiently large parameter space to ensure that our understanding of lifted flame stabilisation is complete. Deliberately simplifying the chemistry model by using single-step global reaction scheme is a way to make the simulation more computationally affordable and thus to span a larger parameter space and ensure that the effect of each parameter is properly understood. The aim of this study is therefore to focus on analysing the structure of a turbulent lifted flame in presence of hot co-flow using a simple-chemistry model. The simulation results presented here will serve as the first of several cases to be studied spanning a range of different conditions.

Governing equations

The conservation equations of mass, momentum, total energy and species are solved in non-dimensional form. These equations are nondimensionalised with respect to the inlet jet width, H , the speed of sound, temperature and thermodynamic properties on the jet centerline at the inlet. For a single-step irreversible reaction of $F + rO \rightarrow (1+r)P$ where r is the stoichiometric ratio, *i.e.* the mass of oxidant disappearing with unit mass of fuel, the non-dimensional system of equations is shown

below,

$$\frac{\partial \rho}{\partial t} + \frac{\partial \rho u_i}{\partial x_i} = 0, \quad (1)$$

$$\frac{\partial \rho u_i}{\partial t} = -\frac{\partial \rho u_i u_j}{\partial x_j} - \frac{\partial p}{\partial x_j} + \frac{\partial \tau_{ij}}{\partial x_j}, \quad (2)$$

$$\frac{\partial \rho E_t}{\partial t} = -\frac{\partial u_j (\rho E_t + p)}{\partial x_j} + \frac{\partial u_j \tau_{ij}}{\partial x_j} - \frac{\partial q_j}{\partial x_j}, \text{ and} \quad (3)$$

$$\frac{\partial \rho Y_k}{\partial t} = -\frac{\partial \rho u_j Y_k}{\partial x_j} + \frac{\partial J_{k,j}}{\partial x_j} + \dot{\omega}_k, \quad k = 1, 2, \quad (4)$$

where ρ is the mixture density, u_i is the velocity vector, Y_k is the mass fraction of the species k , p is the pressure and E_t is the total energy including internal, kinetic, and chemical energies, expressed in non-dimensional form as:

$$E_t = \frac{T}{\gamma} + \frac{1}{2} u_k u_k + \frac{\tau}{Y_{F,st}(\gamma-1)} Y_F. \quad (5)$$

In the above, T is the temperature, γ is the specific heat ratio, $\tau = \alpha/(\alpha-1)$ is the heat release parameter [7], $Y_{F,st}$ is the stoichiometric fuel mass fraction and Y_F is the fuel species mass fraction. The viscous stress tensor, heat flux vector, and species diffusion vector may be expressed as:

$$\tau_{ij} = \frac{\mu}{Re} \left[\frac{\partial u_i}{\partial x_j} + \frac{\partial u_j}{\partial x_i} - \frac{2}{3} \frac{\partial u_k}{\partial x_k} \delta_{ij} \right], \quad (6)$$

$$q_i = -\frac{\mu}{Pr Re} \frac{\partial T}{\partial x_i} - \frac{\tau}{Y_{F,st}(\gamma-1)} J_{k,j}, \text{ and} \quad (7)$$

$$J_{k,j} = \left(\frac{\mu}{Re Sc} \frac{\partial Y_k}{\partial x_i} \right). \quad (8)$$

Variations of viscosity, μ , due to temperature were taken into account by the classical law of $\mu \propto T^{0.75}$ [8]. The non-dimensional form of the ideal gas equation of state is as follows:

$$p = \frac{\gamma-1}{\gamma} \rho T. \quad (9)$$

For a single-step reaction with Arrhenius kinetics, the source terms take the following non-dimensional forms:

$$\dot{\omega}_F = \frac{1}{r} \dot{\omega}_O = -Da \rho^2 Y_F Y_O \exp\left[-\frac{\beta(1-T')}{1-\alpha(1-T')}\right], \text{ and} \\ T' = \frac{(\gamma-1)T-1}{\tau}, \quad (10)$$

where Da is a Damköhler number, α is the heat-release parameter and β is the Zel'dovich factor. The molecular Schmidt number Sc , Prandtl number Pr , Lewis number Le , Reynolds number Re and the flow field parameters are introduced in Table 1.

Numerical methods

Discretisation methods and boundary conditions

The parallel DNS code S3D.SC is used in the present study. The S3D.SC is a modified version of S3D, a FORTRAN code developed in the Combustion Research Facility at Sandia National Laboratories [9]. The modifications have been performed to make the code capable of modelling a simple-chemistry mechanism. The compressible Navier-Stokes, total energy, and species equations are solved on a structured 3D Cartesian mesh. The solver uses high-order accurate, non-dissipative numerical scheme. The spatial derivatives are computed using an 8th order central differencing scheme and the time integration is performed with a 6th stage, 4th order, explicit Runge-Kutta method [10]. To suppress numerical fluctuations at high wave numbers, a 10th filter is applied [11] every 10 time steps. Non-reflecting

Table 1: Numerical and physical parameters of the simulation

	H
Jet width	H
Domain size ($L_x \times L_y \times L_z$)	$20H \times 30H \times 8H$
Number of grid points ($N_x \times N_y \times N_z$)	$1000 \times 1200 \times 400$
Mean inlet jet Mach number (U_j)	0.53
Laminar co-flow Mach number (U_{co})	0.006
Jet non-dimensional temperature	2.5
Co-flow non-dimensional temperature	6.5
Jet Reynolds number	5,300
Inlet velocity fluctuation	10%
Fuel mixture fraction in fuel stream ($Y_{F,o}$)	1.0
Oxidizer mixture fraction in oxidizer stream ($Y_{O,o}$)	1.0
$Y_{F,st}$	0.2
s	4.0
α	0.75
β	6.0
Non-dimensionisation Damköhler number (Da)	4.0
Pr	0.7
Le	1.0

outflow boundary conditions are used in the streamwise and transverse directions [12, 13, 14], and periodic boundary conditions are applied in the spanwise direction.

Flow configuration and simulation parameters

The fuel and oxidizer were injected into the domain separately. The mean inlet axial velocity U_{in} was specified using a *tanh*-based function with a momentum thickness of $0.05H$. The oxidizer had a much lower velocity around 1% of the jet flow and a higher temperature. The fuel was fed into the domain with a frozen turbulent velocity field based on a prescribed turbulent Passot-Pouquet energy spectrum. The domain size, inlet conditions, and chemistry parameters are summarised in Table 1. A uniform grid spacing of $0.02H$ was used in the streamwise and spanwise directions. An algebraically stretched mesh was used in the transverse direction which maintained uniform spacing of $0.02H$ in $|L_y| < 7.5H$ and less than 3% stretching in the region of $|L_y| > 7.5H$. To enable very long-time simulations, a sponge region was used in the transverse direction in the region of $|L_y| > 10H$. In the sponge region, exponential damping terms were added to the governing equations [15]. These prevented instabilities developing where a net transverse velocity drift through the domain existed. The simulation was initially performed on a coarse grid resolution of $0.04H$ for 7.0 flow-jet through times, $\tau_j = L_x/U_j$, to obtain a statistically stationary solution. The solution was then mapped onto a fine grid of $0.02H$ which is approximately two times of the Kolmogorov length scale, which is necessary for good resolution in DNS [18]. The simulation for the fine grid was advanced for $7.0\tau_j$ and the data of the last $5.0\tau_j$ were used for the purpose of analysis.

Results and discussion

Burning mode

Different burning modes in the lifted flame configuration result in complex flame structures. A flame index (FI) representing the degree of mixedness was proposed by Yamashita *et al.* [16] to distinguish premixed from non-premixed flames. The FI is defined as the cosine of oxidizer and fuel gradients as follows:

$$FI = \frac{\nabla Y_F \bullet \nabla Y_O}{|\nabla Y_F| |\nabla Y_O|}. \quad (11)$$

The flame index and mixture fraction Z , defined as

$$Z = \frac{rY_F - Y_O + Y_{O,o}}{rY_{F,o} + Y_{O,o}}, \quad (12)$$

are used to illustrate the global structure of the flame. Three flame elements can be distinguished by using these tools: the

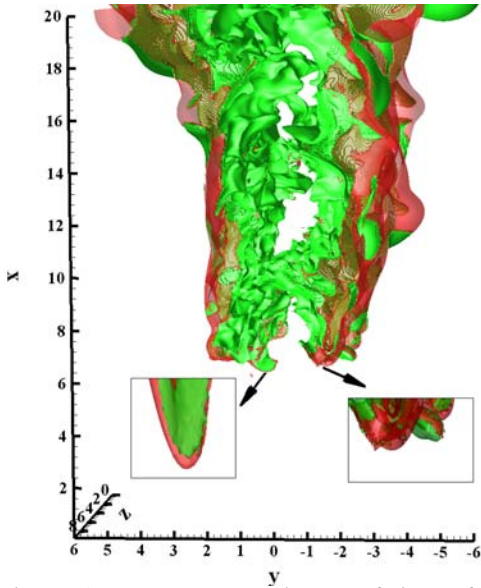


Figure 1: Instantaneous image of iso-surface of non-dimensional temperature $T = 8.0$ coloured by local combustion mode at $t = 12t_j$, red: non-premixed flames and green: premixed flames.

lean premixed wing, the rich premixed wing and a diffusion leading edge flame. Figure 1 shows the iso-surface of non-dimensional temperature $T = 8.0$ which represents approximately 25% of the maximum temperature increase in the domain ($T = T_{co} + 0.25(T_{max} - T_{co})$). This temperature coincides approximately with the maximum reaction rate region. The iso-surface is coloured by flame index according to the different combustion modes that exist. The red colour indicates non-premixed flames with negative flame index and the green colour indicates premixed flames with positive flame index. The flame structure is more complicated compared to quasi-laminar triple flames presented in the literature. The flame is essentially composed of a shrouding, quasi-laminar non-premixed flame existing at the outer edges of the jet, with a highly turbulent rich premixed flame in the jet core. In this respect, the structure is similar to the lifted flame studied by Mizobuchi *et al.* [4]. However, only non-premixed flames were observed in the region just upstream of the flame base. The PDF of the FI at the flame base is shown in Figure 2. The results show that probability of the situation in which FI is negative is about 75 %, indicating the stabilisation is essentially non-premixed.

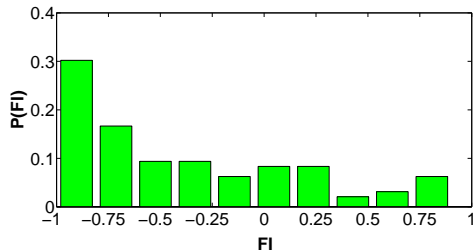


Figure 2: PDF of the flame index evaluated at the flame base.

Flame base analysis

The scalar dissipation rate can be used to examine the rate of molecular mixing. The scalar dissipation rate is defined as,

$$\chi = 2D|\nabla Z|^2, \quad (13)$$

where D is the diffusion coefficient of the mixture fraction. The scalar dissipation rate is the key parameter in many models for turbulent non-premixed combustion. If scalar dissipation is close to the ignition or extinction limits, experimental and theoretical studies show that dissipation effects can play an important role in determining the stabilisation location [17].

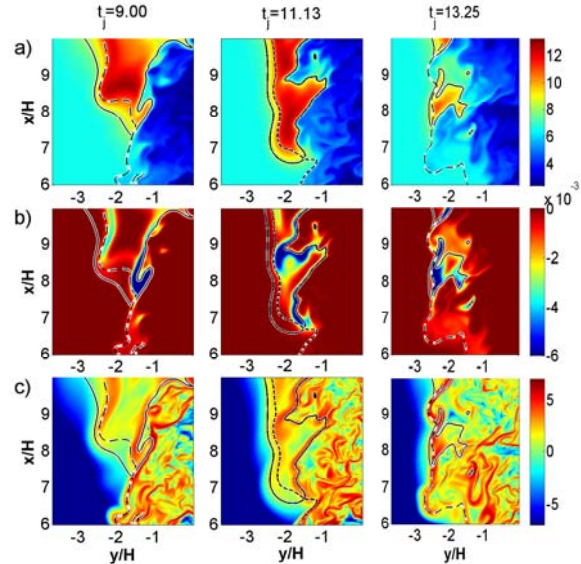


Figure 3: Temporal snapshot of a) temperature, b) reaction rate and c) log of scalar dissipation rate at the flame base (the solid line is non-dimensional temperature iso-line of 8.0 and the dash line is the most reactive mixture fraction iso-line of 0.13).

Auto-ignition of stagnant adiabatic mixtures with initial condition and chemistry presented in Table 1 was simulated to find the shortest homogeneous ignition delay corresponding to most reactive mixture fraction, Z_{MR} [19], which is around 0.13 in this study. The flame base is then identified as the intersection of this most reactive mixture fraction Z_{MR} iso-surface and the temperature iso-surface of $T = T_{co} + 0.25(T_{max} - T_{co})$. Figure 3 shows a contour plot at three time instants of temperature, reaction rate and scalar dissipation rate at the flame base. It can be concluded that the flame base which is the location with a high reaction rate can be tracked quite well with the intersection of temperature and most reactive mixture fraction iso-lines. Because of the high turbulence levels, unlike the previous studies of mixing layers [2, 3], the flame base does not have triple-flame shape: the wings of the triple flame are essentially merged as shown in Figure 3(b). Inspection of the scalar dissipation structures in Figure 3(c) shows that the lean flame branch and trailing diffusion flame is quasi-laminar, with only minor fluctuations of scalar dissipation present. In contrast, the inner rich premixed flame experiences significant fluctuations of dissipation rate, indicating that it exists in a much more turbulent region.

Figure 4 shows scatter plots, collected in time, of temperature and product mass fraction versus mixture fraction at different streamwise locations. As expected, the temperature is very close to the mixing line and mass fraction of product is almost zero at $x/H = 2.0$ indicating that no reaction has occurred yet. Close to the flame base, $x/H = 6.5$, there is an increase in temperature and mass fraction of products centered on the most reactive mixture fraction. Finally at $x/H = 12.0$, the temperature and product mass fraction progressively approach their adiabatic equilibrium level on the lean side, while on the rich side evidence of ongoing ignition or broad premixed flame zones still exists.

Visual analysis of the flame base shows that the flame base is pushed upstream as the flow velocity is higher than propagation speed of the flame base, meanwhile a pocket of auto-ignitable fuel and oxidizer mixture is auto-ignited just downstream of the flame base and is then convected upstream once more. This sequential behaviour has been observed over time in both sides of the jet shear layers. Statistical analysis of key parameters like edge flame position and its displacement speed is necessary to further understand the flame base physics. This is left for future work.

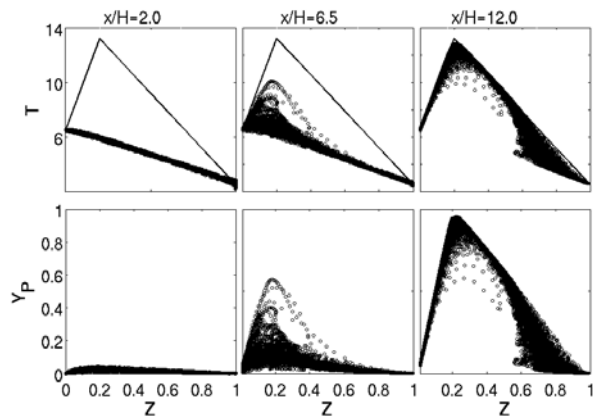


Figure 4: Time cumulative scatter plots of temperature and product mass fraction as a function of mixture fraction at different streamwise locations. The solid line is obtained from the Burke and Schumann solution.

Conclusions

Three-dimensional DNS of a turbulent lifted slot jet flame in a hot co-flow was performed using single-step chemistry with a Reynolds number of 5300. The flame structure was analysed using a flame index (FI) to mark whether the combustion mode was premixed or non-premixed. The overall structure of the flame consisted of a quasi-laminar diffusion flame shrouding a highly turbulent inner premixed flame. At the flame base, diffusion flames were more prominent, indicating the stabilisation was essentially non-premixed. Superimposing temperature and the most reactive mixture fraction iso-lines on reaction rate and scalar dissipation rate showed that the intersection of these two iso-lines is a good marker of the flame base. As the reaction rate maxima regions coincide with the most reactive mixture fraction, it can be concluded that auto-ignition was the main reason of stabilisation given the present parameter set. Further work is planned to consider a wider range of parameters and to study the flame stabilisation in greater detail.

Acknowledgements

This work was supported by the Australian Research Council under grant number DP110104764. This research was undertaken on the NCI National Facility in Canberra, Australia, which is supported by the Australian Commonwealth Government.

References

- [1] Navarro-Martinez, S. and Kronenburg, A., Analysis of stabilisation mechanisms in lifted flames, *AIP Conference Proceedings*, **13**, 2009, 13–38.
- [2] Nichols, W. N. and Schmid, P. J., The effect of a lifted flame on the stability of round fuel jet, *Journal of Fluid Mechanics*, **609**, 2008, 275–284.
- [3] Jiménez, C. and Cuenot, B., DNS study of stabilisation of turbulent triple flames by hot gases, *Proceedings of the Combustion Institute*, **31**, 2007, 1649–1656.
- [4] Mizobuchi, Y., Shinjo, J., Ogawa, S. and Takeno, T., A numerical study on the formation of diffusion flame islands in a turbulent hydrogen jet lifted flame, *Proceedings of the Combustion Institute*, **30**, 2005, 611–619.
- [5] Yoo, C. S., Sankaran, R. and Chen, J. H., Three-dimensional direct numerical simulation of a turbulent

lifted hydrogen jet flame in heated coflow: flame stabilisation and structure, *Journal of Fluid Mechanics*, **640**, 2009, 453–481.

- [6] Yoo, C. S., Richardson, E. S., Sankaran, R. and Chen, J. H., A DNS study on the stabilisation mechanism of a turbulent lifted ethylene jet flame in highly-heated coflow, *Proceedings of the Combustion Institute*, **33**, 2011, 1619–1627.
- [7] Chakraborty, N. and Mastorakos, E., Direct numerical simulations of localised forced ignition in turbulent mixing layers: the effects of mixture fraction and its gradient, *Flow Turbulence Combustion*, **80**, 2008, 155–186.
- [8] Pantano, C., Direct simulation of non-premixed flame extinction in a methane air jet with reduced chemistry, *Journal of Fluid Mechanics*, **514**, 2004, 231–270.
- [9] Chen, J. H., Choudhary, A., De Supinski, B., Devries, M., Hawkes, E. R., Klasky, S., Liao, W. K., Ma, K. L., Mellor-Crummey, J., Podhorski, N., Sankaran, R., Shende, S., Yoo, C. S., Terascale direct numerical simulations of turbulent combustion using S3D, *Computational Science and Discovery*, **2**, 2009.
- [10] Kennedy, C. A., Carpenter, M. H. and Lewis, R. M., Low-storage, explicit Runge-Kutta schemes for the compressible Navier-Stokes equations, *Applied Numerical Mathematics*, **35**, 2000, 117–219.
- [11] Kennedy, C. A. and Carpenter, M. H., Several new numerical methods for compressible shear-layer simulations, *Applied Numerical Mathematics*, **14**, 1994, 397–433.
- [12] Sutherland, J. C. and Kennedy, C. A., Improved boundary conditions for viscous, reacting, compressible flows, *Journal of Computational Physics*, **19**, 2003, 502–524.
- [13] Yoo, C. S., Wang, Y., Trouvé, A. and Im, H. G., Characteristic boundary conditions for direct numerical simulations of turbulent counterflow flames, *Combustion Theory Modelling*, **9**, 2005, 617–646.
- [14] Yoo, C. S. and Im, H. G., Characteristic boundary conditions for simulations of compressible reacting flows with multi-dimensional, viscous and reaction effects, *Combustion Theory Modelling*, **11**, 2007, 259–286.
- [15] Stanley, S. A., Sarkar, S. and Mellado, J. P., A study of the flow-field evolution and mixing in a planar turbulent jet using direct numerical simulation, *Journal of Fluid Mechanics*, **450**, 2002, 377–407.
- [16] Yamashita, H., Shimada, M. and Takeno, T., A numerical study of flame stability at the transition point of jet diffusion flames, *Twenty-Sixth Symposium (International) on Combustion/ The Combustion Institute*, 1996, 27–34.
- [17] Pitsch, H. and Fedotov, V., Stochastic modeling of scalar dissipation rate fluctuations in non-premixed turbulent combustion, *Center for Turbulence Research, Annual Research Briefs*, 2000, 91–103.
- [18] Pope, S. B., *Turbulent Flows*, Cambridge University Press, 2000.
- [19] Mastorakos, E., Baritaud, T. A. and Poinot, T. J., Numerical simulations of autoignition in turbulent mixing flows, *Combustion and Flame*, **109**, 1997, 198–223.